Lab on a Chip

PAPER

View Article Online
View Journal | View Issue

Cite this: *Lab Chip*, 2018, **18**, 335

Electrochemical biosensor for cancer cell detection based on a surface 3D micro-array†

Li An,[a] Guangtong Wang, *[a] Yu Han, [b] Tianchan Li,[a] Peng Jin*[b] and Shaoqin Liu *[a]

Received 16th October 2017,
Accepted 6th December 2017

DOI: 10.1039/c7lc01117b

rsc.li/loc

The detection of rare circulating tumour cells (CTCs) in patients' blood is crucial for the early diagnosis of cancer, highly precise cancer therapy and monitoring therapeutic outcomes in real time. In this study we have developed an efficient strategy to capture and detect CTCs from the blood of cancer patients using a benzoboric acid modified gold-plated polymeric substrate with a regular 3D surface array. Compared with the smooth substrate, the substrate with the surface 3D microarrays exhibited a higher capture efficiency, *i.e.* 3.8 times that afforded by the smooth substrate. Additionally, due to the reversible reaction between the benzoboric acid on the 3D microarray and the sialic acid on CTCs, our strategy allowed for easy detachment of the captured CTCs from the substrate without causing critical damage to the cells. This will be of benefit for gaining further access to these rare cells for downstream characterization. The proposed strategy provides several advantages, including enhanced capture efficiency, high sensitivity, low cost and recovery of isolated CTCs, and could become a promising platform for early stage diagnosis of cancer.

Introduction

Cancer is one of the serious threats to the health of human beings nowadays and it restricts the improvement of humans' living quality. Along the roadmap to highly precise and personalized cancer therapy, the development of selectively detecting, isolating and quantifying cancer biomarkers and circulating tumour cells (CTCs) in circulation are important ongoing areas. Early diagnosis of cancer is crucial to reduce high lethality and patient spending, since cancer is much easier to be cured in early stages.[1] Circulating tumour cells[2–5] (CTCs) are one of the important indexes of cancer progression and prognosis. CTCs have long been considered a reflection of tumour aggressiveness because haematogenous spreading of CTCs may not only give rise to metastases in distant organs, but also be capable of self-seeding back to their original organs.[6,7] The detection of CTCs in the blood of cancer patients can be used for early diagnosis of cancers, evaluation of cancer prognosis, real-time monitoring therapeutic outcomes and understanding the biological mechanisms underlying metastasis.[2–5] Therefore, it is quite urgent to develop new methods to detect circulating tumor cells with easy operation, high efficiency and low cost. However, the isolation and subsequent profiling of CTCs remains a challenge because: (1) the concentration of CTCs in the bone marrow or blood is as low as one CTC in 10^6 to 10^7 white blood cells and 10^9 red blood cells. (2) The presence of other cellular contaminants, including epidermal cells, other normal epithelial cells and circulating blood cells, may also introduce significant interference. Therefore, CTC detection requires extremely sensitive and specific analytical methods. In the last several decades, numerous efforts have been made to develop a reliable method to detect and quantify CTCs in peripheral blood, and various CTC analysis platforms have been developed, including reverse transcriptase polymerase chain reaction (RT-PCR),[8–10] flow cytometry,[11,12] fibre-optic array scanning technology (FAST),[13,14] microfluidic systems,[15–17] nanoparticle-assisted systems[18–20] and so on.[21,22] The CellSearch system is the only CTC product approved by the FDA for CTC based cancer diagnosis in patients with breast, prostate, and metastatic colorectal cancers, which provides prognostic value in cancer patients.[23,24] Most of these techniques still require a pre-enrichment step to make the sensitivity reach an acceptable level. The pre-enrichment step, for example immunomagnetic bead enrichment, will make the operation of the detection more complicated and increase the cost. Moreover, CTCs captured by most techniques are nonviable and could not be recovered for downstream characterization.[25–28] Therefore, a CTC detection platform

[a] *State Key Laboratory of Urban Water Resource and Environment, Harbin Institute of Technology, Harbin 150090, China. E-mail: shaoqinliu@hit.edu.cn, wgt@hit.edu.cn*
[b] *Center of Ultra-precision Optoelectronic Instrument, Harbin Institute of Technology, Harbin 150080, China. E-mail: P.Jin@hit.edu.cn*

† Electronic supplementary information (ESI) available. See DOI: 10.1039/c7lc01117b

which can combine an enrichment procedure with CTC detection and facilitate the recovery of the captured CTCs for subsequent characterizations might allow us to overcome some of the above-mentioned challenges.

In this study, we utilized a benzoboric acid modified gold-plated polymeric substrate with a regular 3D surface array to isolate and release cancer cells from all blood. Application of this approach provided the following advantages: (a) unlike commonly used flat surfaces modified with antibodies (such as EpCAM) for CTC capturing, a 3D microarray was fabricated on the substrate using a nanoimprinting technique. The nanostructured substrates increased the surface area for biomolecule binding and cancer cell adhesion,[29–34] thus significantly enhancing CTC capture efficiency. In addition, compared with other techniques, such as corrosion, electrochemical deposition, and chemical vapor deposition,[32] the pattern of the 3D surface microarray fabricated using the nanoimprinting technique was much more regular, controllable and robust, making detection more repeatable. (b) The 3D microarray was coated with gold layers which allowed the combination of enrichment with direct detection by electrochemical impedance spectroscopy (EIS).[35–40] (c) As shown in Scheme 1, the gold-plated 3D microarray was then modified by organic molecules containing a benzoboric acid group, which can reversibly bind with the vicinal diol structure in the sialic acid molecule exclusively overexpressed on the cytomembrane of cancer cells.[41–43] Herein the use of the benzoboric acid group instead of antibodies, which are commonly used to capture cancer cells,[44,45] not only reduced the cost of the enrichment process, but also made the platform easier to be preserved because small organic molecules are much cheaper and more robust than antibodies. (d) The reversible interaction between benzoboric acid and the vicinal diol structure in sialic acid (Scheme 1) can be readily disrupted under mild conditions in the presence of excess sialic acid, resulting in the release of CTCs from the surface for subsequent cell analysis.[46,47] It was found that the proposed approach can specifically detect cancer cells in a blood sample and its detection limit was as low as 5 cells per mL without any pre-enrichment. Consequently, our work offers a simple, rapid and sensitive approach for detecting, isolating, and quantifying CTCs in blood specimens at low concentration.

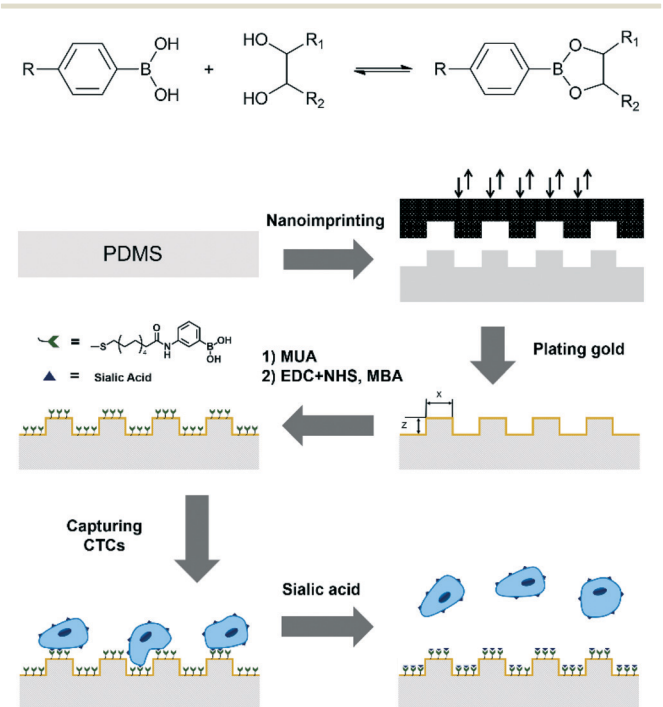

Scheme 1 Design of an MBA modified gold-plated polymeric substrate with a regular 3D surface array for the capture, detection and release of CTCs.

Experimental

Materials and methods

The gold-plated polymeric material was provided by the National Centre for Nanoscience and Technology of China. 11-Mercaptoundecanoic acid (MUA) was purchased from Sigma-Aldrich. 3-Aminophenylboronic acid (MBA), *N*-3-(dimethylaminopropyl)-*N*′-ethylcarbodiimide hydrochloride (EDC), *N*-hydroxysuccinimide (NHS) and inorganic salts were purchased from J&K Tech. All aqueous solutions were prepared using ultrapure water (18.2 MU, Milli-Q, Millipore). Human whole blood was purchased from the Hospital of Harbin Institute of Technology.

The surface morphology of the 3D microarray was investigated using a scanning electron microscope (SEM) (Hitachi S-4800, Japan) operating at an accelerated voltage of 10 kV. The contact angle was measured using a Jc2000D2 contact angle meter, Shanghai Zhongchen Digital Technic Apparatus Co., Ltd. X-ray photoelectron spectra (XPS) were measured using an Escalab 205Xi X-ray photoelectron spectrometer. Electrochemical experiments were carried out with a three-electrode system comprising a platinum count electrode, a Ag/AgCl reference electrode and the modified working electrode with the surface 3D microarray. Electrochemical impedance spectroscopy (EIS) was performed using a Solartron 1260A Impedance/Gain-phase Analyser (UK). All the impedance spectra were recorded within the frequency range of 0.1 Hz–100 kHz at a 0 V bias potential. The amplitude of the applied sine wave potential in each case was 10 mV.

Fabrication of the gold-plated 3D microarray

A 3D microarray was fabricated on a polymeric substrate using a nanoimprinting technique as shown in Scheme 1. Firstly, a mould with the designed pattern as shown in Table S1† was prepared by photolithography. Then the pattern was transferred onto the polymeric substrate by the nanoimprinting technique. A series of the 3D arrays with different morphologies was fabricated. A 20 nm Cr layer and a 100 nm Au layer were successively deposited on the surface of the substrate by magnetron sputtering as shown in Scheme 1.

Modification of the gold-plated 3D microarray

The benzoboric acid groups were introduced on the 3D gold-plated microarray by the following steps. The gold-plated 3D microarray was immersed in an ethanol solution of 10 mM MUA for 24 h after cyclic voltammetric scanning in 0.5 M H_2SO_4. Thus, MUA could bind onto the 3D array *via* the Au–S interaction. The 3D array was then immersed into the activation solution (45 mM EDC and 15 mM NHS in PBS buffer) for 1 h to activate the carboxyl groups. After rinsing with water, the 3D array was immersed in a H_2O/MeOH solution containing 10 mM MBA for 24 h to allow the MBA to covalently bind on MUA. The modified 3D microarray was stored at −4 °C prior to use.

Cell culture

Human breast carcinoma cells (MCF-7), human lung adenocarcinoma cells (A549) and human umbilical vein endothelial cells (HUVEC) were purchased from the cell library of the Chinese Academy of Sciences. HUVEC were cultured in DMEM medium (Thermo Scientific) supplemented with 10% fetal bovine serum (FBS; heat-inactivated; Thermo Scientific) and 100 μg mL^{-1} penicillin–streptomycin (Thermo Scientific) in a 5% CO_2 atmosphere at 37 °C. MCF-7 and A549 cells were cultured in RPMI 1640 medium (Thermo Scientific) supplemented with 10% fetal bovine serum (FBS; heat-inactivated; Thermo Scientific) and 100 μg mL^{-1} penicillin–streptomycin (Thermo Scientific) in a 5% CO_2 atmosphere at 37 °C. After culturing for 24 h, the cells were collected and separated from the medium by centrifugation at 800 rpm for 3 min, and were then washed twice with a sterile PBS solution (pH 7.2). The cell sediment was trypsin-dispersed to obtain a homogeneous cell suspension, which was then diluted to a suitable concentration by PBS. The cell number was determined using a Petroff–Hausser cell counting chamber.

Cell capturing of the 3D microarray

The substrate with the 3D microarray was cut into 5 mm × 5 mm square pieces and immersed in the cell suspension. Then they were stored in a 5% CO_2 atmosphere at 37 °C for 15 min, 30 min, 45 min, 60 min or 90 min for capturing cells from the suspension. The substrate with the 3D microarray was afterwards washed by PBS three times to remove nonspecific adsorbate. For observation, the cells captured on the 3D array were fixed by paraformaldehyde solution and stained with 4′6-diamidino-2-phenylindole (DAPI). The cells absorbed on the 3D array were observed using an Olympus fluorescence microscope.

Detection of MCF-7 in whole blood

MCF-7 cells were respectively spiked into healthy human whole blood with cell concentrations of approximately 1 × 10^5, 5 × 10^4, 1 × 10^4, 5 × 10^3, 1 × 10^3, 5 × 10^2, 1 × 10^2, 50, 10, 5, and 0 cells per mL. The 3D array was immersed in whole blood samples containing different densities of MCF-7 cells in a 5% CO_2 atmosphere at 37 °C for 60 min. Then the 3D array was washed with PBS five times to remove the materials and cells physically absorbed on the 3D array. MCF-7 detection was carried out by EIS using these 3D arrays with cells attached as the working electrode. The electrolyte for EIS is composed of 5 mM $[Fe(CN)_6]^{3-/4-}$ and 5 mM PBS.

Results and discussion

Characterization of the MBA modified gold-plated polymeric substrate with a regular 3D surface array

The benzoboric acid modified, gold-plated polymeric substrate with a regular 3D surface array that we fabricated was confirmed by SEM as shown in Fig. 1a and Fig. S1–S5.† It could be found that 3D microarrays with different morphologies were successfully fabricated on the polymeric substrate and exhibited good stability even after being immersed in H_2O/MeOH for 24 h (Fig. S6†). Then we followed sequential chemical functionalization routes to modify the benzoboric acid groups on the gold-plated 3D microarray. The gold-plated 3D microarray was first functionalized with MUA though a Au–thiol reaction. Then the MBA was covalently grafted onto MUA after the MUA was activated by EDC and NHS. The successful modification of the 3D array with MBA was confirmed by EIS, XPS and contact angle characterizations. As shown in Fig. 1b, remarkable semicircle portions of the different electrodes are observed, and the electron-transfer resistance (R_{ct}) is about 155.7 Ω for the bare gold-plated 3D microarray. After being functionalized with MUA, R_{ct} of the electrode greatly increased to 748.1 Ω, because the negatively-charged MUA molecules hindered the electron transfer of the redox probes. However, when MBA was covalently attached to the MUA-modified gold-plated 3D

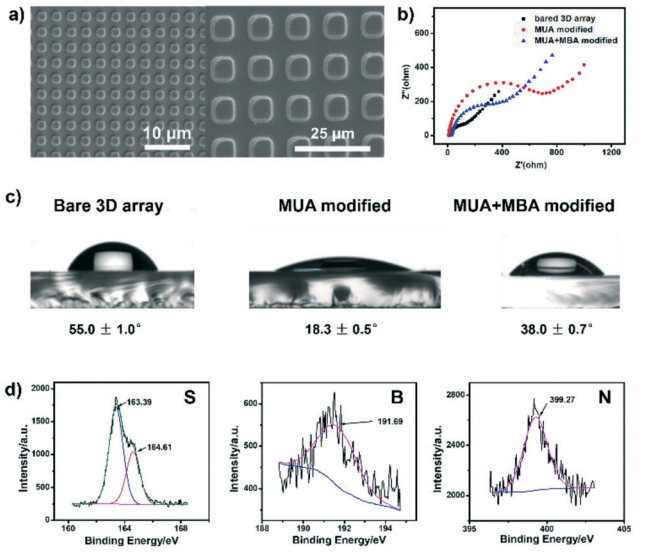

Fig. 1 a) SEM images of the gold-plated 3D array. b) Nyquist plots of the gold-plated 3D microarray before and after modification. c) Modification of the gold-plated 3D microarray characterized by contact angles. d) Characterization of S, B and N on the 3D microarray using XPS.

microarray, R_{ct} of the electrode slightly decreased to 507.4 Ω. This can be attributed to the K_a value of boric acid, which is lower than that of the carboxyl group in MUA. In the meantime, each step of the modification was also confirmed by contact angle measurement. As shown in Fig. 1c, the contact angle of the 3D array decreased from 55.0 ± 1.0° to 18.3 ± 0.5° after the modification of MUA, indicating that the MUA-modified gold-plated 3D microarray was more hydrophilic due to the existence of the carboxyl group. After binding MBA, the contact angle increased back to 38.0 ± 0.7° owing to poorer hydrophilicity of the benzoboric acid group. In addition, as shown in Fig. S7a,† the characteristic peaks of Au (Au 4f7/2 84.0 eV and Au 4f5/2 87.7 eV), S (S2p 163.39 eV and 164.61 eV), B (B1s 191.69 eV), and N (N1s 191.69) can be found in the XPS of the modified 3D microarray. In the Au 4f region, there are two gold bands $4f_{7/2}$ and $4f_{5/2}$, which occur at 84.0 ± 0.2 eV and 87.7 ± 0.2 eV (Fig. S7b†), respectively, corresponding to bulk evaporated gold. Deconvolution of the sulfur (2p) spectrum reveals two doublets with binding energies of 163.39 eV and 164.61 eV (Fig. 1d). These peaks are assigned to the $2p_{3/2}$ and $2p_{1/2}$ spin–orbit split levels, which are consistent with chemisorbed MUA molecules, indicating the presence of a metal–thiolate bond. The spectra for the B and N regions are all consistent with the presence of MBA molecules (Fig. 1d). The above results indicate the successful fabrication of the 3D microarray as well.

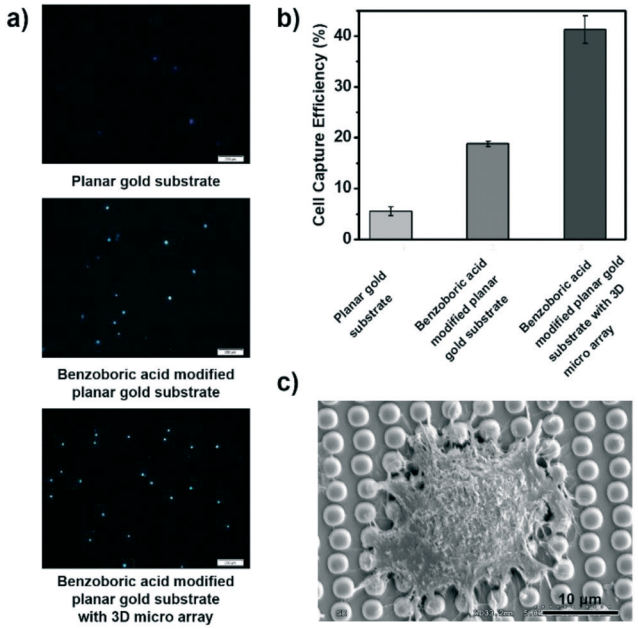

Fig. 2 Enhanced cell capture using an MBA modified gold-plated polymeric substrate with a regular 3D surface array: a) quantification of captured MCF-7 cells on the smooth gold-plated polymeric substrate, MBA modified smooth gold-plated polymeric substrate and MBA modified gold-plated polymeric substrate with a regular 3D surface array. Scale bar is 200 μm for all images. b) The relative cell capture efficiencies for the assay corresponding to a). c) SEM image of the captured MCF-7 cells on the MBA modified gold-plated polymeric substrate with a regular 3D surface array.

Cell capture

To start with we verified the contribution of the benzoboric acid film and the 3D microarray towards cell capture, using the MCF-7 cell line. The benzoboric acid modified gold-plated polymeric substrate with a regular 3D surface array was compared with the smooth gold-plated polymeric substrate and the benzoboric acid modified smooth gold-plated polymeric substrate. The MCF-7 cancer cell line was soaked in PBS to obtain a cell loading of 1×10^4 cells per mL and was then incubated with different substrates for 60 min. After cell capture, the substrates were rinsed with PBS and the cells captured by the substrates were stained with DAPI and observed by fluorescence microscopy. Fig. 2a shows fluorescence images of different substrates after capturing MCF-7 cells. It can be observed that negligible cells were captured in the case of the smooth gold-plated polymeric substrate. However, in the case of the benzoboric acid modified smooth gold-plated polymeric substrate and benzoboric acid modified gold-plated polymeric substrate with the regular 3D surface array, we can observe that the cell capture efficiency increased (Fig. 2b), which is evidenced in the images by a greater degree of fluorescence density of the captured cells. The SEM image in Fig. 2c shows the morphology of MCF-7 which attaches onto the benzoboric acid modified gold-plated polymeric substrate with a regular 3D surface array. These observations indicate that benzoboric acid groups and the 3D structure play essential roles as a capture agent for the specific binding of cells and as a template for benzoboric acid grafting, respectively.

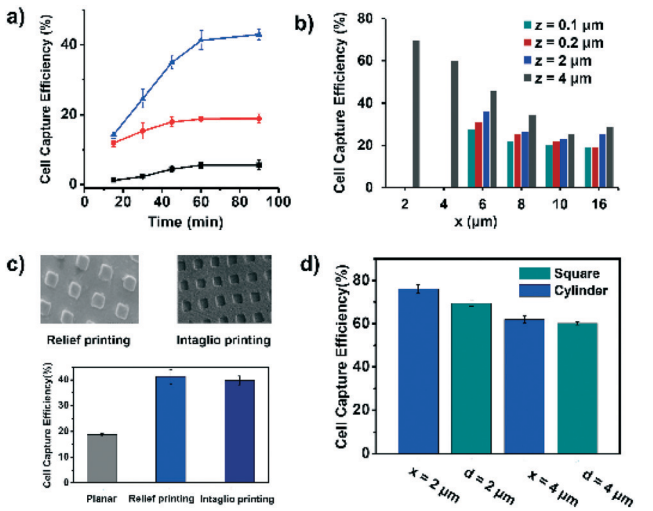

Fig. 3 a) Optimization of the capture time of the flat substrate (black), benzoboric acid modified flat substrate (red) and benzoboric acid modified substrate with 3D microarray (blue). b) The cell capture efficiencies of the 3D microarrays with different size (x) and depth (z). c) The cell capture efficiencies of the intaglio printing 3D microarray and the relief printing 3D microarray, where x = 0.5 μm and z = 0.2 μm. d) The capture efficiencies of the square 3D microarray and the cylindrical 3D microarray, where z = 2.0 μm.

Following this, we investigated the effect of incubation time and the morphology of the 3D microarray on capture efficiency. We first investigated the effect of incubation time on capture efficiency. As shown in Fig. 3a, the correlated increase in the capture efficiency of MCF-7 cells with the incubation time can be observed up to 60 min, but the capture efficiency was saturated over 60 min. Therefore, 60 min was selected as the optimum incubation time in the following study. Secondly, as shown in Fig. 3b, it was found that the morphology of the 3D microarray can influence the cell capture efficiency significantly. In general, the cell capture efficiency increased with the increase of the depth (z) or the decrease of size (x) of the 3D microarray (setting of parameters x and z is shown Scheme 1). In addition, as shown in Fig. 3c and d, the shape of the 3D microarray also has a slight effect on the capture efficiency. Finally, we found that the cylindrical 3D microarray with a diameter of 2 μm and depth of 2 μm had the highest capture efficiency in our experiments. The efficiency was as high as 76%, which is 3.8 times that of the MBA modified smooth gold-plated polymeric substrate. Therefore, the cylindrical 3D microarray with a diameter of 2 μm and depth of 2 μm was selected to prepare the working electrode of the biosensors in the following study.

Performance evaluation of the benzoboric acid modified gold-plated polymeric substrate with the regular 3D surface array

Firstly, we tested the specificity of the benzoboric acid modified gold-plated polymeric substrate with the regular 3D surface array to capture CTCs using MCF-7 and A549 cancer cell lines as model CTCs, and compared it with a control case using the HUVEC normal cell line as a negative control. Different cell lines were soaked in PBS to obtain suspensions with 10^4 cells per mL and the cells were captured by the 3D microarray. It was found that only 6.7% HUVEC was captured by the 3D microarray, which is much lower than that of MCF-7 and A549 (76% and 64%). Higher capture efficiencies of the MCF-7 and A549 cancer cell lines can be attributed to the overexpression of sialic acid on the surface of MCF-7 and A549 cells.

Secondly, we further tested the ability of the MBA modified gold-plated polymeric substrate with the regular 3D surface array to capture cells from fresh whole blood samples. 10^4 per mL MCF-7 cells stained with DiD were dispersed into human whole blood. After capture by the substrate, all captured cells on the 3D array were stained with DAPI. From the bright field image in Fig. 4b, we observed that negligible red blood cells were captured by the 3D microarray. According to the fluorescence images in Fig. 4b, nearly all the cells on the 3D microarray emitted both blue and red fluorescence, confirming that only MCF-7 cells and not white blood cells were captured. This result further suggested that the cells that do not overexpress sialic acid are unable to attach to the substrate in this approach.

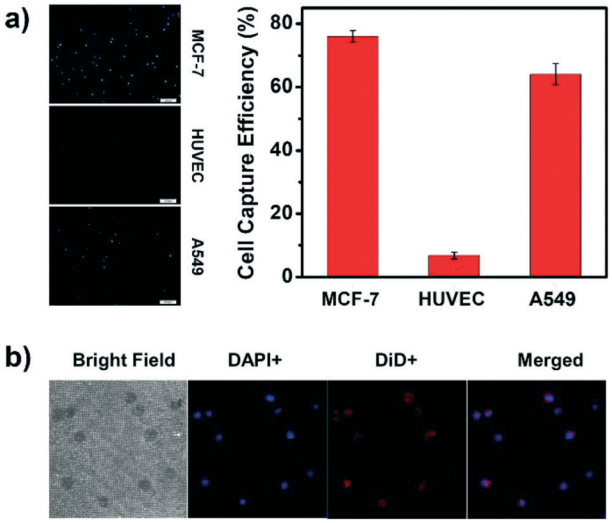

Fig. 4 a) The capture efficiency of MCF-7, HUVEC and A549 cells. The concentrations of the cell suspensions were all 10^4 per mL. b) Fluorescence images of the cell capture by the 3D array in a blood sample.

The 3D microarray was coated with gold layers and could be used as the working electrode of the EIS biosensor. This means that our approach can combine cell capture with direct detection of CTCs using the EIS technique. The number of CTCs present in patients' blood can be highly variable. To evaluate the capture sensitivity of the MBA modified gold-plated polymeric substrate with the regular 3D surface array at varying concentrations of cancer cells, we added MCF-7 cancer cells into whole blood at concentrations ranging from 5 to 10^5 cells per mL. Fig. 5a shows Nyquist plots of the benzoboric acid modified gold-plated polymeric substrate with the regular 3D surface array after incubation with varying concentrations of cancer cells. It was found that the diameter of the semicircle portions of the electrodes increased with increasing MCF-7 cell concentrations. A linear correlation between the relative impedance, R_{ct}/R_0, and the logarithmic value of cell concentration was observed as shown in Fig. 5b. The linear regression equation was R_{ct}/R_0 = 0.5081 log[$C_{MCF\text{-}7}$] + 0.0304 with a correlation coefficient (R^2) of 0.9857. The detection limit was as low as 5 cells per mL,

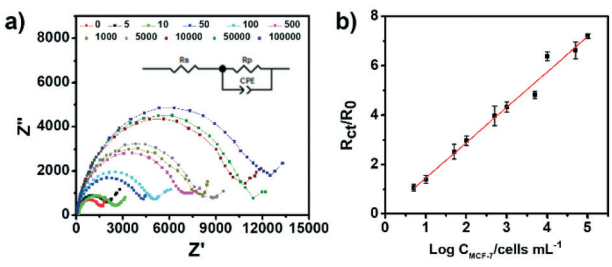

Fig. 5 a) The EIS spectra of the prepared biosensor at different concentrations of MCF-7 cells. The inset shows the equivalent circuit for the EIS measurement. b) The relationship between the concentration of MCF-7 cells and the impedance of the prepared EIS biosensor.

Table 1 A comparative table of the performance parameters of recently reported platforms for cancer cell detection

Detection method	Limit of detection (cells per mL)	Reproducibility	Ref.
Chemiluminescence	1×10^4	5.36%	48
Cyclic voltammetry	4.41×10^3	2%	49
EIS	20	—	36
Surface-enhanced Raman scattering	5	—	50
Cyclic voltammetry	15	5.6%	51
Cyclic voltammetry	3.3×10^2	6.4%	35
EIS	10	6%	38
EIS	10	2.09%	39
EIS	10	1.75–3.69%	40
EIS	5	1.7%	This study

which was better than most other biosensors based on EIS for cancer cell detection (Table 1).

Release of MCF-7 cells captured by the MBA modified gold-plated polymeric substrate with the regular 3D surface array

Based on the exchange reaction illustrated in Scheme 1, the binding between the benzoboric acid on the substrate and the sialic acid on the cytomembrane of cancer cells can be readily disrupted by adding excess sialic acid, resulting in the release of isolated CTCs from the substrate for subsequent cell analysis. We incubated the attached CTCs with 20 mM sialic acid for 30 min and investigated the release efficiency and the viability of the recovered cancer cells. Fig. 6a shows the fluorescence images of MCF-7 cancer cells on the benzoboric acid modified substrate with the regular 3D surface array before and after sialic acid treatment. It was found that the substrate exhibited good cell detachment performance, with a release efficiency of 97% for MCF-7 cancer cell lines. In the meantime, as shown in Fig. 6b, the viability of the released cells was determined to be 98% by the double staining technique. The released cells were subsequently cultured in DMEM high glucose medium for 2 days. As shown in Fig. 6c and Fig. S8,† the cells detached from the substrate can proliferate rapidly, further indicating that viability of the released cells is still maintained. The retention of the cell viability will benefit subsequent analysis of the released cells greatly.

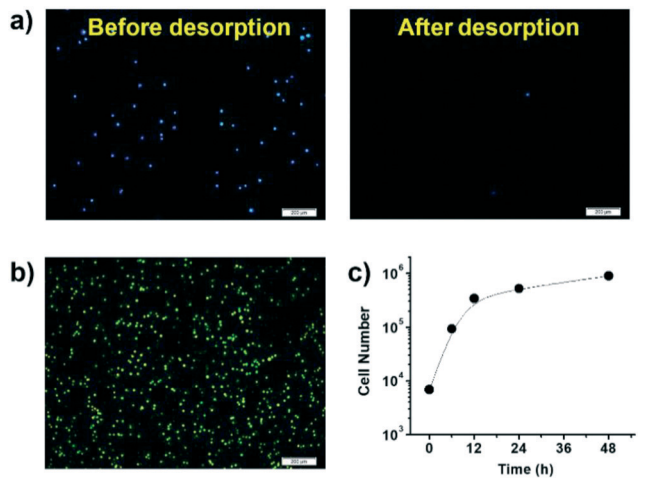

Fig. 6 a) Desorption of cells. b) The viability of released cells characterized by double staining. c) The proliferation of the MCF-7 cells that detached from the 3D microarray.

Conclusions

We have demonstrated an alternative strategy to efficiently isolate cancer cells from whole blood using a benzoboric acid modified gold-plated polymeric substrate with a regular 3D surface microarray. The introduction of the 3D microarray significantly enhanced the capture efficiency of cancer cells. By combining with the EIS technique, the substrate we prepared could be used for the direct detection of cancer cells in whole blood samples, and the detection limit of the biosensor was as low as 5 cells per mL. Moreover, using the substrate we prepared, the isolated cancer cells can be recovered through simple exchange reactions without significant damage. Thanks to the ease of fabrication, accurate structural control over the electrode surfaces, and high sensitivity and specificity towards the target cells, the present method may provide a promising platform for early stage diagnosis of cancer and downstream characterization. Although the CTC capture efficiency of the current device is not satisfactory enough, it can be further improved by combining a microarchitecture embedded microfluidic chip with the current device, which can improve cell–interface interactions and facilitate the processing of patient blood samples.[45,52]

Conflicts of interest

There are no conflicts to declare.

Acknowledgements

We thank Pengchao Zhang from the Institute of Chemistry, Chinese Academy of Science for helpful discussion. This research was financially supported by the National Natural Science Foundation of China (grant no. 51372054), the Open Project of State Key Laboratory of Urban Water Resource and Environment, Harbin Institute of Technology (No. ES201703), the Fundamental Research Funds for the Central Universities (Grants No. HIT – NSRIF-201703) and the Open Project of Key Laboratory of Micro-Systems and Micro-Structures

Manufacturing of Ministry of Education, Harbin Institute of Technology (Grant No. 2016KM009).

Notes and references

1 J. W. Uhr, *Nature*, 2007, **450**, 1168.
2 W. J. Allard, J. Matera, M. C. Miller, M. Repollet, M. C. Connelly, C. Rao, A. G. J. Tibbe, J. W. Uhr and L. W. M. M. Terstappen, *Clin. Cancer Res.*, 2004, **10**, 6897.
3 Z. Y. Shen, A. G. Wu and X. Y. Chen, *Chem. Soc. Rev.*, 2017, **46**, 2038.
4 S. K. Arya, B. Lim and A. R. A. Rahman, *Lab Chip*, 2013, **13**, 1995.
5 V. Plaks, C. D. Koopman and Z. Werb, *Science*, 2013, **341**, 1186.
6 M. Y. Kim, T. Oskarsson, S. Acharyya, D. X. Nguyen, X. H. F. Zhang, L. Norton and J. Massague, *Cell*, 2009, **139**, 1315.
7 B. J. Green, T. S. Safaei, A. Mepham, M. Labib, R. M. Mohamadi and S. O. Kelley, *Angew. Chem., Int. Ed.*, 2016, **55**, 1252.
8 A. Fabisiewicz, J. Kulik, P. Kober, E. Brewczynska, T. Pienkowski and J. A. Siedlecki, *Acta Biochim. Pol.*, 2004, **51**, 747.
9 A. E. Ring, L. Zabaglo, M. G. Ormerod, I. E. Smith and M. Dowsett, *Br. J. Cancer*, 2005, **92**, 906.
10 T. J. Molloy, L. A. Devriese, H. H. Helgason, A. J. Bosma, M. Hauptmann, E. E. Voest, J. H. M. Schellens and L. J. van't Veer, *Br. J. Cancer*, 2011, **104**, 1913.
11 M. Takao and K. Takeda, *Cytometry, Part A*, 2011, **79**, 107.
12 L. L. Wang, Y. Y. Wang, Y. J. Liu, M. Cheng, X. Wu and H. M. Wei, *J. Exp. Clin. Cancer Res.*, 2009, **28**, 88.
13 H. B. Hsieh, D. Marrinucci, K. Bethel, D. N. Curry, M. Humphrey, R. T. Krivacic, J. Kroener, L. Kroener, A. Ladanyi, N. Lazarus, P. Kuhn, R. H. Bruce and J. Nieva, *Biosens. Bioelectron.*, 2006, **21**, 1893.
14 R. T. Krivacic, A. Ladanyi, D. N. Curry, H. B. Hsieh, P. Kuhn, D. E. Bergsrud, J. F. Kepros, T. Barbera, M. Y. Ho, L. B. Chen, R. A. Lerner and R. H. Bruce, *Proc. Natl. Acad. Sci. U. S. A.*, 2004, **101**, 10501.
15 S. Nagrath, L. V. Sequist, S. Maheswaran, D. W. Bell, D. Irimia, L. Ulkus, M. R. Smith, E. L. Kwak, S. Digumarthy, A. Muzikansky, P. Ryan, U. J. Balis, R. G. Tompkins, D. A. Haber and M. Toner, *Nature*, 2007, **450**, 1235.
16 L.-Yu Hung, C.-H. Wang, C.-Yu. Fu, P. Gopinathan and G.-B. Lee, *Lab Chip*, 2016, **16**, 2759.
17 J. Che, V. Yu, E. B. Garon, J. W. Goldman and D. D. Carlo, *Lab Chip*, 2017, **17**, 1452.
18 M. M. Costa, A. Escosura-Muñiz, C. Nogués, L. Barrios, E. Ibáñez and A. Merkoçi, *Nano Lett.*, 2012, **12**, 4164.
19 M. Perfézou, A. Turner and A. Merkoçi, *Chem. Soc. Rev.*, 2012, **41**, 2606.
20 M. Espinoza-Castañeda, A. Escosura-Muñiz, A. Chamorro, C. Torres and A. Merkoçi, *Biosens. Bioelectron.*, 2015, **67**, 107.
21 J. F. Swennenhuis, A. G. J. Tibbe, R. Levink, R. C. J. Sipkema and L. W. M. M. Terstappen, *Cytometry, Part A*, 2009, **75**, 520.
22 D. Antolovic, L. Galindo, A. Carstens, N. Rahbari, M. W. Büchler, J. Weitz and M. Koch, *BMC Biotechnol.*, 2010, **10**, 35.
23 M. Cristofanilli, G. T. Budd, M. J. Ellis, A. Stopeck, J. Matera, M. C. Miller, J. M. Reuben, G. V. Doyle, W. J. Allard, L. W. M. M. Terstappen and D. F. Hayes, *N. Engl. J. Med.*, 2004, **351**, 781.
24 S. J. Cohen, C. J. A. Punt, N. Iannotti, B. H. Saidman, K. D. Sabbath, N. Y. Gabrail, J. Picus, M. Morse, E. Mitchell, M. C. Miller, G. V. Doyle, H. Tissing, L. W. M. M. Terstappen and N. J. Meropol, *J. Clin. Oncol.*, 2008, **26**, 3213.
25 W. Zhao, C. H. Cui, S. Bose, D. Guo, C. Shen, W. P. Wong, K. Halvorsen, O. C. Farokhzad, G. S. L. Teo, J. A. Phillips, D. M. Dorfman, R. Karnik and J. M. Karp, *Proc. Natl. Acad. Sci. U. S. A.*, 2012, **109**, 19626.
26 A. M. Shah, M. Yu, Z. Nakamura, J. Ciciliano, M. Ulman, K. Kotz, S. L. Stott, S. Maheswaran, D. A. Haber and M. Toner, *Anal. Chem.*, 2012, **84**, 3682.
27 M. Labib, B. Green, R. M. Mohamadi, A. Mepham, S. U. Ahmed, L. Mahmoudian, I.-H. Chang, E. H. Sargent and S. O. Kelley, *J. Am. Chem. Soc.*, 2016, **138**, 2476.
28 W. Li, E. Reátegui, M.-H. Park, S. Castleberry, J. Z. Deng, B. Hsu, S. Mayner, A. E. Jensen, L. V. Sequist and S. Maheswaran, *Biomaterials*, 2015, **65**, 93.
29 C. J. Bettinger, R. Langer and J. T. Borenstein, *Angew. Chem., Int. Ed.*, 2009, **48**, 5406.
30 P. C. Zhang, L. Chen, T. L. Xu, H. L. Liu, X. L. Liu, J. X. Meng, G. Yang, L. Jiang and S. T. Wang, *Adv. Mater.*, 2013, **25**, 3566.
31 X. Yao, R. Peng and J. D. Ding, *Adv. Mater.*, 2013, **25**, 5257.
32 P. C. Zhang and S. T. Wang, *ChemPhysChem*, 2014, **15**, 1550.
33 X. L. Liu and S. T. Wang, *Chem. Soc. Rev.*, 2014, **43**, 2385.
34 Y.-Q. Li, B. K. Chandran, C. K. Lim and X. D. Chen, *Adv. Sci.*, 2015, **2**, 1500118.
35 T. Li, Q. Fan, T. Liu, X. Zhu, J. Zhao and G. Li, *Biosens. Bioelectron.*, 2010, **25**, 2686.
36 Y. K. Chung, J. Reboud, K. C. Lee, H. M. Lim, P. Y. Lim, K. Y. Wang, K. C. Tang, H. Ji and Y. Chen, *Biosens. Bioelectron.*, 2011, **26**, 2520.
37 Z. J. Zhang, L. Wu, J. S. Wang, J. S. Ren and X. G. Qu, *Chem. Commun.*, 2013, **49**, 9986.
38 Y. Liu, F. J. Zhu, W. X. Dan, Y. Fu and S. Q. Liu, *Analyst*, 2014, **139**, 5086.
39 H. W. Shen, J. Yang, Z. P. Chen, X. P. Chen, L. Wang, J. Hu, F. H. Ji, G. M. Xie and W. L. Feng, *Biosens. Bioelectron.*, 2016, **81**, 495.
40 M. Dervisevic, M. Senel, T. Sagir and S. Isik, *Biosens. Bioelectron.*, 2017, **90**, 6.
41 J. A. Peters, *Coord. Chem. Rev.*, 2014, **268**, 1.
42 X. Wu, Z. Li, X.-X. Chen, J. S. Fossey, T. D. Jamesc and Y.-B. Jiang, *Chem. Soc. Rev.*, 2013, **42**, 8032.
43 H. L. Liu, Y. Y. Li, K. Sun, J. B. Fan, P. C. Zhang, J. X. Meng, S. T. Wang and L. Jiang, *J. Am. Chem. Soc.*, 2013, **135**, 7603.
44 S. Hou, H. C. Zhao, L. B. Zhao, Q. L. Shen, K. S. Wei, D. Y. Suh, A. Nakao, M. A. Garcia, M. Song, T. Lee, B. Xiong, S.-C. Luo, H.-R. Tseng and H.-H. Yu, *Adv. Mater.*, 2013, **25**, 1547.

45 H. J. Yoon, A. Shanker, Y. Wang, M. Kozminsky, Q. Jin, N. Palanisamy, M. L. Burness, E. Azizi, D. M. Simeone, M. S. Wicha, J. S. Kim and S. Nagrath, *Adv. Mater.*, 2016, **28**, 4891.
46 A. Matsumoto, N. Sato, K. Kataoka and Y. Miyahara, *J. Am. Chem. Soc.*, 2009, **131**, 12022.
47 H. Otsuka, E. Uchimura, H. Koshina, T. Okano and K. Kataoka, *J. Am. Chem. Soc.*, 2003, **125**, 3493.
48 W. Liu, H. Wei, Z. Lin, S. Mao and J. Lin, *Biosens. Bioelectron.*, 2011, **28**, 438.
49 M. D. Costa, A. D. L. Escosura-Muñiz, C. Nogués, L. Barrios, E. Ibáñez and A. Merkoçi, *Small*, 2012, **8**, 3605.
50 X. Wu, L. Luo, S. Yang, X. Ma, Y. Li, C. Dong, Y. Tian, L. Zhang, Z. Shen and A. Wu, *ACS Appl. Mater. Interfaces*, 2015, **7**, 9965.
51 D. Sun, L. Jing, Y. Zhong, Y. Yu, Y. Wang, B. Zhang and Z. Chen, *Biosens. Bioelectron.*, 2016, **75**, 301.
52 J. Wu, Q. S. Chen and J. M. Lin, *Analyst*, 2017, **142**, 421.

